INTERNATIONAL JOURNAL OF ENGINEERING AND MANAGEMENT SCIENCES
© 2004-13 Society For Science and Nature (SFSN), All Rights Reserved
www.scienceandnature.org

LASER BEAM INDUCED CURRENT (LBIC) INSTRUMENTATION FOR SEMICONDUCTOR RESEARCH

Kulkarni Gururaj Anand
S.D.M.C.E.T., Dharwad, Karnataka, India

ABSTRACT
Operational capabilities of a cost effective indigenously developed Laser Beam Induced Current (LBIC) instrumentation have been demonstrated. For the low temperature LBIC measurements a continuous flow Liquid Helium cryostat has been fabricated indigenously and its operability has been tested. Preliminary LBIC imaging data collected on HgCdTe epitaxial layer grown on CdZnTe and Si solar cell devices have been presented, to demonstrate the operability of the LBIC system.

KEYWORDS: Laser Beam Induced Current (LBIC), HgCdTe, CdZnTe,

INTRODUCTION

It is well known that the spatial inhomogeneities in semiconductor starting materials severely affect the uniformity in performance of the final opto-electronic devices fabricated on those materials [1]. In particular, II-VI HgCdTe grown on CdZnTe is the best example for this class of materials, since HgCdTe is known to be defective semiconductor [2]. The non-uniformities in the HgCdTe starting material limits the final focal plane array (FPA) operability, which has become a stringent requirement for both strategic and tactical applications[1,3]. Diagnostic techniques that reveal spatially resolved material characteristics (structural, electrical or optical) with a spatial resolution smaller than the eventual device size are therefore necessary to identify the root causes of these spatial variations, and for material screening and growth/process optimization prior to costly and time consuming device processing. However, prior screening of these semiconductors used for subsequent device fabrication is limited by the lack of adequate diagnostic techniques. It is in this context that Laser Beam Induced Current (LBIC) experimentation has been presented here as a characterization tool for the cause.

Back Ground Theory for LBIC

Laser-Beam-Induced-Current (LBIC) is a high-resolution, non-destructive optical characterization technique used to spatially map and identify charge separating regions associated with electrically active regions and defects in semiconductors and devices [1, 3]. In the LBIC technique, a low power laser is focused onto the semiconductor wafer creating localized electron-hole pairs. In a uniform defect-free material, these electron-hole pairs would naturally recombine within a diffusion length resulting in the absence of any lateral photovoltaic effect and hence no current flow between two remote contacts. On the other hand, the presence of any electric fields, associated with electrically active regions within a few diffusion lengths of the photogenerated carriers, would separate the electron-hole pairs and induce a lateral photovoltaic effect which causes a current to flow between the remote contacts. By scanning the laser beam across the sample, a two-dimensional LBIC image can be generated which represents the spatial distribution of any electrically active charge separating regions within the semiconductor [4].

When applied to unprocessed materials, the LBIC image represents the spatial distribution of various electrically active charge separating regions which may be associated with inclusions, strain, damage, precipitates, stacking faults, twin boundaries, dislocation clusters, bandgap and doping variations, etc [4].

A p-n junction is a special case of an electrically active region in a semiconductor and is a simple structure whose charge separating effects are well understood. Figure 1 demonstrates the differences in sample configuration for the normal photovoltaic response, and the LBIC response. In a standard photovoltaic response measurement, contacts are made on each side of the junction (contacts A and C) and the current is measured between these contacts as a function of the position of the laser beam. A line scan of this current, as the beam is scanned across the p-n junction, is shown in figure 1. By contrast, for LBIC measurements, both the contacts are made on the p-side (contacts A and B) and a line scan of this current, as the laser beam is scanned across the p-n junction, shows the characteristic bipolar behavior depicted in figure 1. The bipolar signal is a result of no bias being applied between the contacts; therefore, there is no preferred direction of current flow. If the carriers are generated in the center of the p-n junction, equal currents will flow in both the directions, resulting in zero net current. As the beam is scanned away from the center in both directions, the net current, though equal in magnitude, flows in opposite directions. This bipolar response is an especially distinctive and advantageous feature of LBIC in contrast to conventional photovoltaic response where contact made directly to the device results in a unipolar response [1]. The orientation and magnitude of the LBIC signal are dependent on both the geometry and junction type, as well as on the relative position and orientation of the photodiode with respect to the two remote contacts [4].

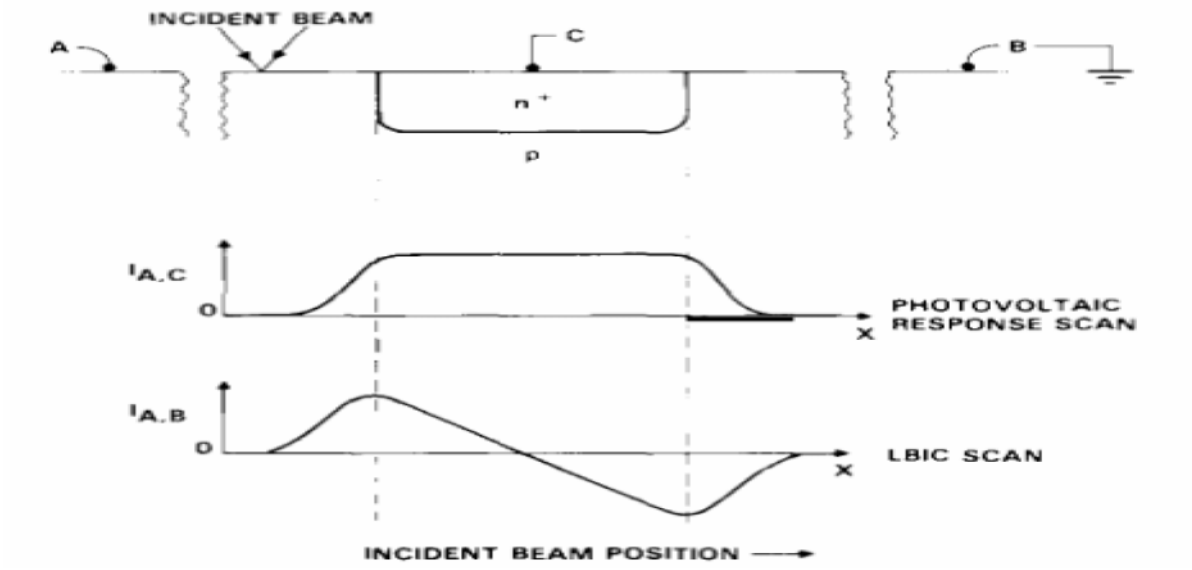


Figure 1: Optoelectronic response of a p-n junction contrasting photovoltaic response and LBIC [1].

If there is an array of p-n junctions in the sample, the photovoltaic response measurement would require a contact to each element of the array. In contrast, the LBIC measurement requires only two contacts at two remote ends to scan all the individual elements of the array. Therefore LBIC offers a unique way of studying the opto-electronic behavior of each element in the array without requiring contacts to individual elements of the array [1].

LBIC Experimental Setup

Figure 2 shows an experimental setup for laser beam induced current (LBIC) measurements. Laser beam from the diode laser having the wavelength of 670 nm with 3 mW power is chopped using Model SR540 chopper controller. The reference frequency (R_f) from SR540 is given to the reference frequency terminal of the Lock-in-Amplifier. The chopped laser beam is focused onto the sample using the microscope objective and reflecting mirror. The sample is moved under the fixed laser beam on computer-controlled X, Y translation stages having a minimum step size of 1.25 μm and can scan a maximum distance of 25 mm.

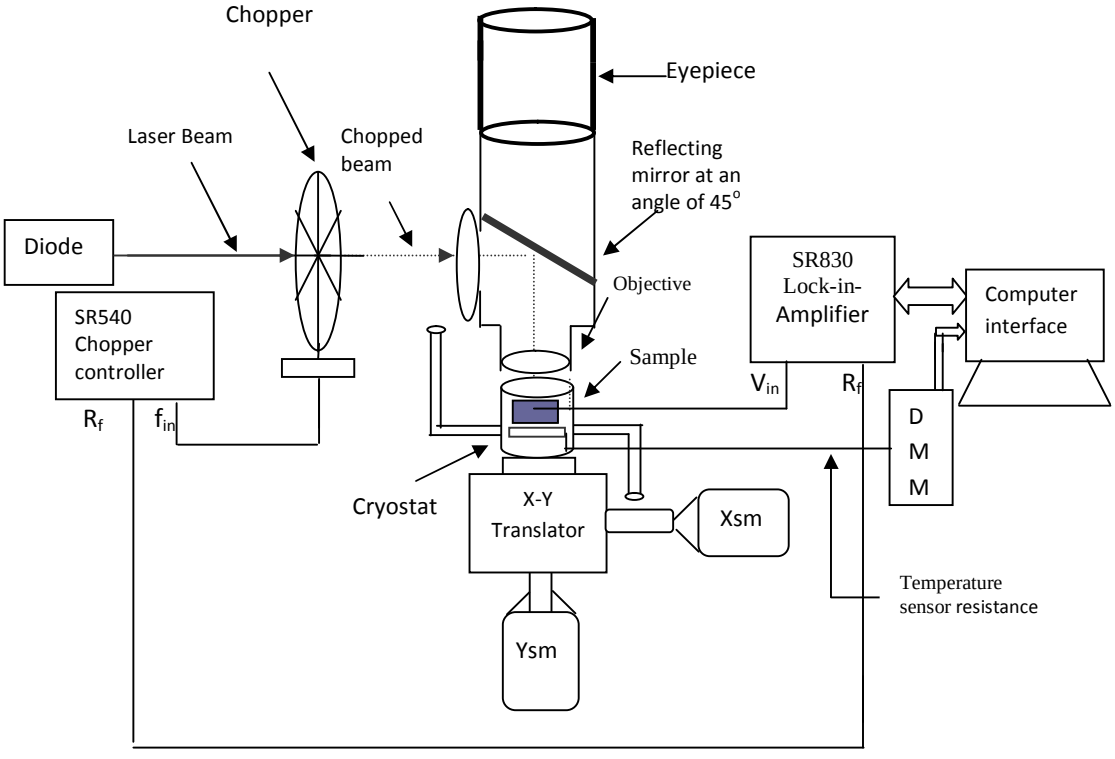


Figure 2: LBIC experimental setup

The photo-generated current is converted to photo voltage V_{in} and is measured by the Lock-in-Amplifier and sent to an acquisition card. The numerical photo voltage value for each point is stored in a data file, together with all relevant measurement parameters. The Data acquisition is done with IEEE – 488.2 GPIB. This X-Y translator stage can be controlled both manually and with the computer system.

SOME PRELIMINARY LBIC MEASUREMENTS

(I) On Si Solar Cells

A silicon solar cell is a large area device (shown in figure 3) whose global I-V characteristics and efficiency strongly depend on the local properties. The existence of local defects may adversely influence the solar cell global properties. Experimental techniques suitable to map the spatial distribution of such local defects can provide valuable information, and thus help to improve the technology for production of efficient and reproducible solar cells. The LBIC (Light Beam Induced Current) is a well known technique for mapping of the spatial distribution of the photo current of a solar cell leading to analysis of such defects.

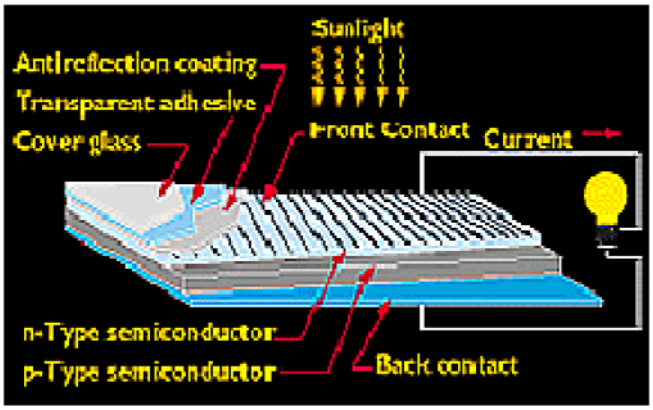
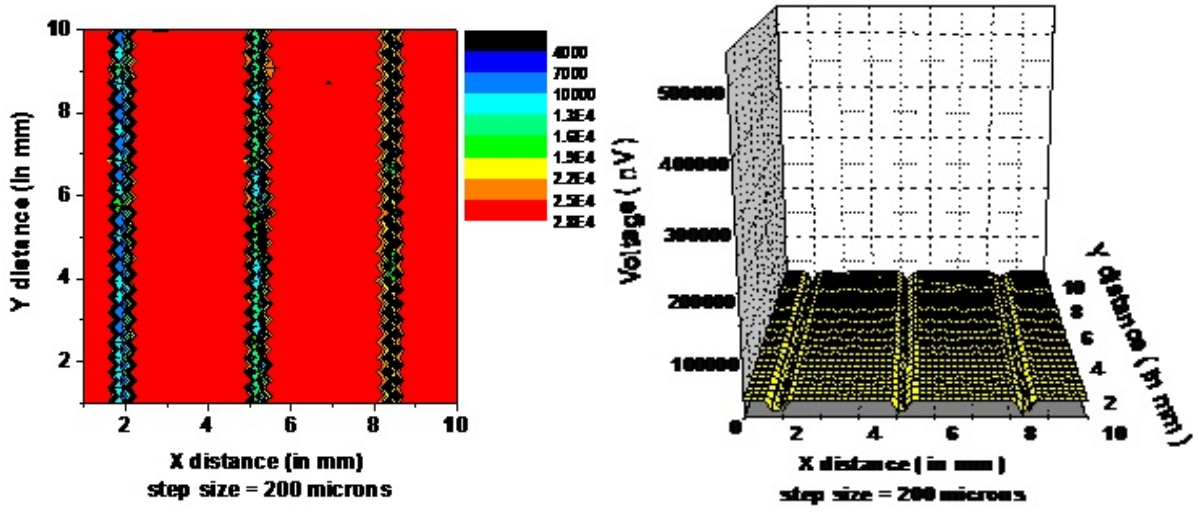


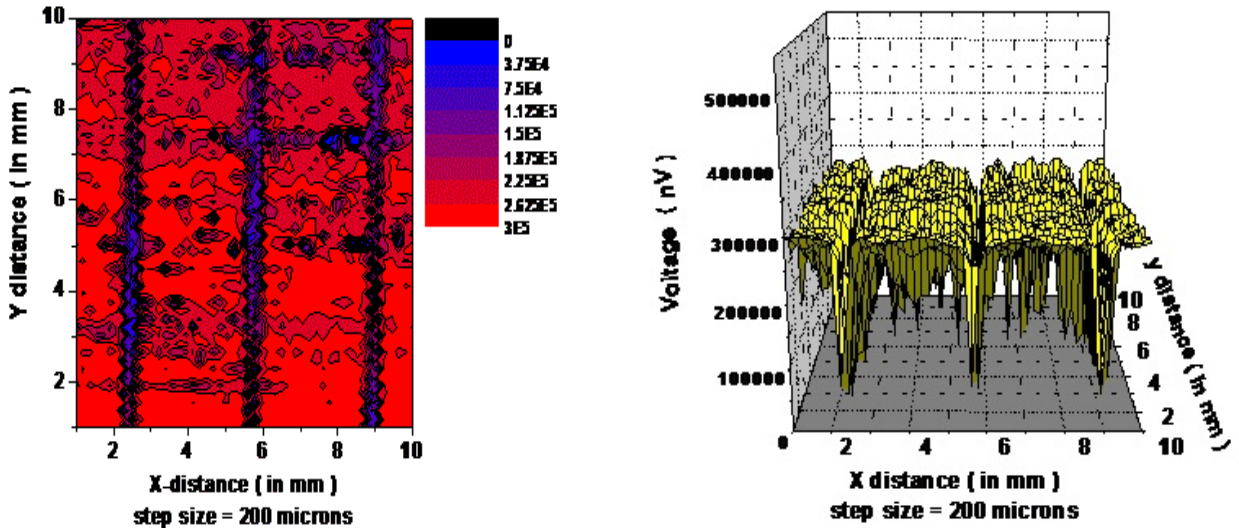
Figure 3: A typical solar cell panel illustrating the principle of operation

The following are some of the LBIC maps taken on three different types of Si solar cells supplied by Bharat Heavy Electrical Limited (BHEL), Bangalore; namely ER-type, C-type and E-type. From the LBIC measurements on these solar cells, it is found that ER-type solar cell photo voltage is too low (~ 20μV) when it is compared to the C and E type solar cells. So the ER-type solar cell is called an electrically rejected solar cell. For the C –type solar cell, the photo voltage lies between 300 - 450 μV, where as for the E-type solar cell the photo voltage is between 500-600 μV.



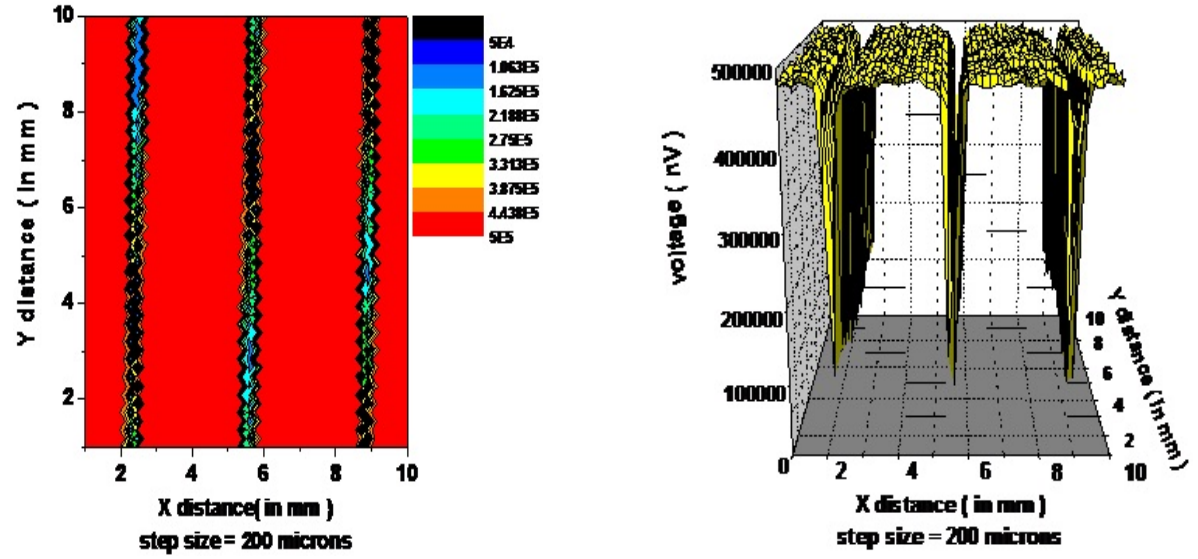
(i) **(ii)**

Figure 3(a): LBIC images of the ER-type solar cell (i) 2D image (ii) 3D image



(i) **(ii)**

Figure 3(b): LBIC images of the C-type solar cell (i) 2D image (ii) 3D image

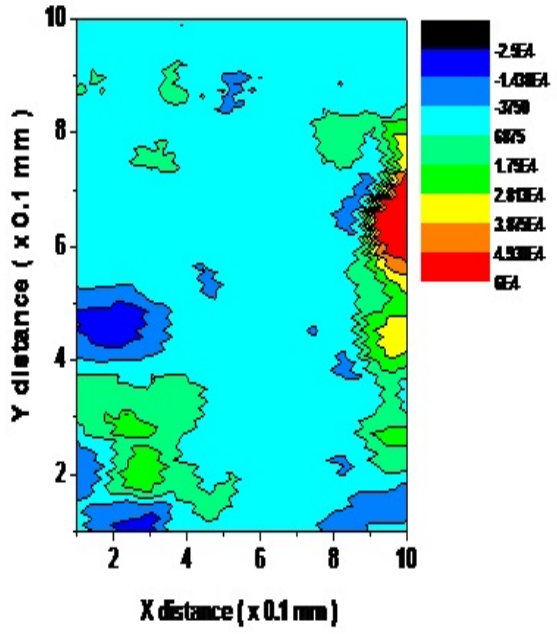


(i) **(ii)**

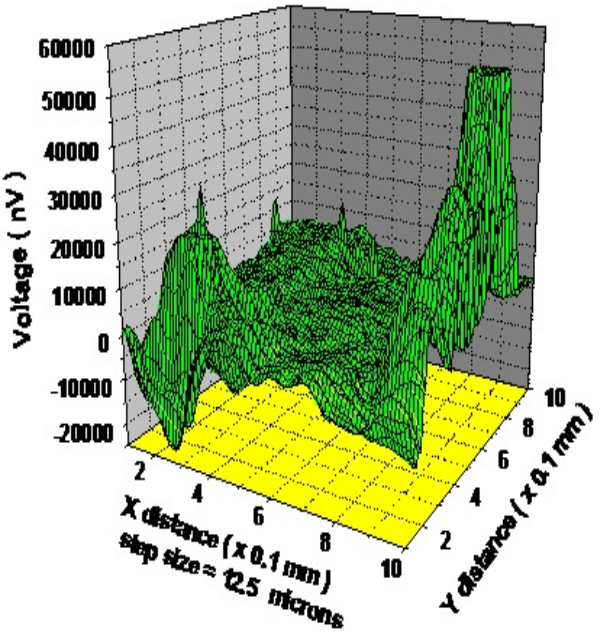
Figure 3(c): LBIC images of the E-type solar cell (i) 2D image (ii) 3D image

(II) On HgCdTe Epitaxial Layers

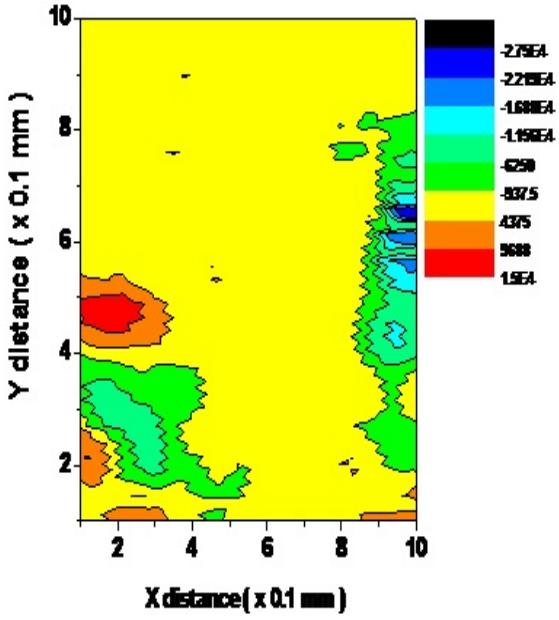
It is well known that $Cd_{0.96}Zn_{0.04}Te$ material remains the substrate of choice for epitaxial growth of HgCdTe for use in high performance infrared (IR) detectors and focal plane arrays (FPAs) [5]. The performance of these HgCdTe-based IR FPAs can be limited by the non-uniformities in the performance of the individual detectors. This variation in performance may be caused either by pre-existing spatial inhomogeneities in the HgCdTe starting material, or may be introduced during device fabrication by any one of the device processing steps [1, 3]. Therefore prior screening of HgCdTe epilayers can reduce the cost of the final device. LBIC is the best technique to map the non-uniformities in the as grown HgCdTe epitaxial layers grown on the CdZnTe substrates. Figures 4(a) and 4(b) show the LBIC maps for HgCdTe epitaxial layers grown on CdZnTe substrates. These maps may be representing the spatial distribution of various electrically active charge separating regions, which may be associated with defects. For complete understanding of these maps, the full defect modeling needs to be done which in turn needs the understanding of defects in the substrates, their impact during the growth of HgCdTe (or MCT) epitaxial layers and the effects of subsequent post growth treatments like annealing on the as grown HgCdTe epitaxial layers. Since the objective here is to demonstrate the operational capabilities of the LBIC system, only the preliminary data collected using this instrument are presented.



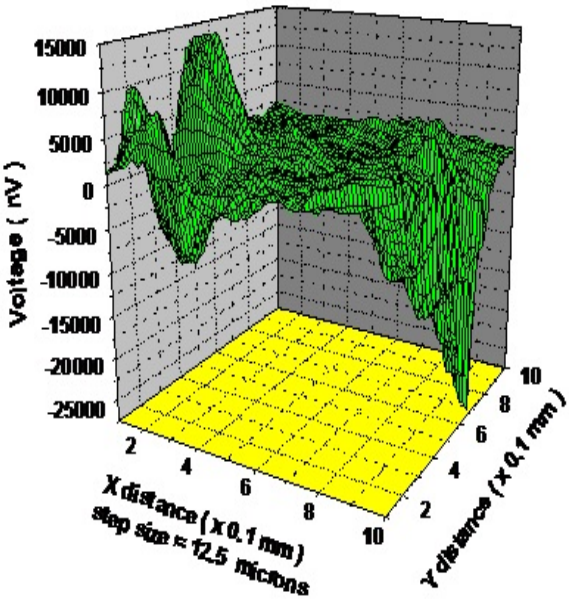
(i)



(ii)

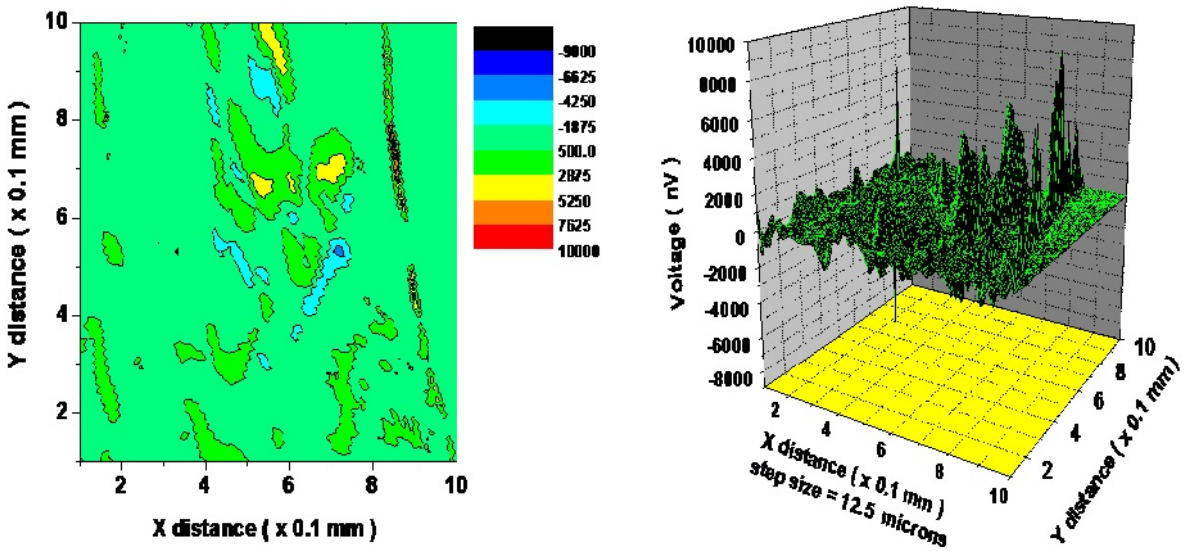


(iii)



(iv)

Figure 4(a): LBIC images of MCT epitaxial layer (i) 2D image and (ii) 3D image taken at 90K, (iii) 2D image and (iv) 3D image taken at 110K



(i) **(ii)**

Figure 4(b): LBIC images of MCT epitaxial layer (i) 2D image and (ii) 3D image taken at room temperature

CONCLUSIONS

In summary the operational capabilities of the indigenously developed LBIC system have been demonstrated, along with the arrangement for the low temperature LBIC measurements, using the liquid helium cryostat designed and fabricated for the cause.

ACKNOWLEDGEMENT

I acknowledge Prof. K.S.R.K. Rao of semiconductor laboratory, Department of Physics, I.I.Sc., Bangalore for allowing me to work for the fabrication LBIC system and subsequent measurements. I also acknowledge S.S.P.L., Delhi and B.H.E.L., Bangalore for the samples.

BIBLIOGRAPHY

[1] J. Bajaj and W.E. Tennant, J. Cryst. Growth **103**, 170 (1990).

[2] S. Sitharaman, R. Raman, L. Durai, S. Pal, M. Gautam, A. Nagpal, S. Kumar, S. N. Chatterjee, and S. C. Gupta, J. Cryst. Growth **285,** 318 (2005).

[3] J. Bajaj, W.E. Tennant, R. Zucca and S.J.C. Irvine, Semicond. Sci. Technol. **8**, 872 (1993).

[4] K.A. Fynn, J. Bajaj and L. Faraone, IEEE transactions on electron devices **42(10)**, 1775 (1995).

[5] G.A.Kulkarni, V.G. Sathe, K.S.R.K. Rao, D.V.S. Muthu and R.K. Sharma, J. Appl. Phys. **105,** 063512 (2009) and the references there in.